Electronic Supplementary Material (ESI) for Journal of Materials Chemistry B.

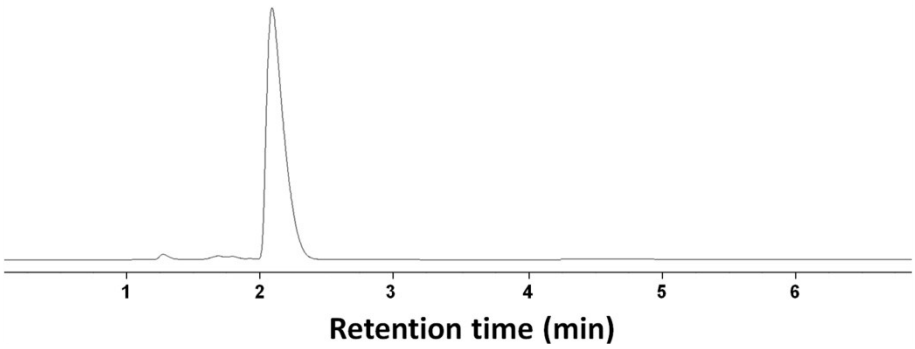

Fig. S1. HPLC trace for purified ADD-DOX conjugates. The mobile phase was water/methanol/acetic acid (11/88/1, v/v/v). The purity of ADD-DOX was determined to be 96.7% by peak integration.

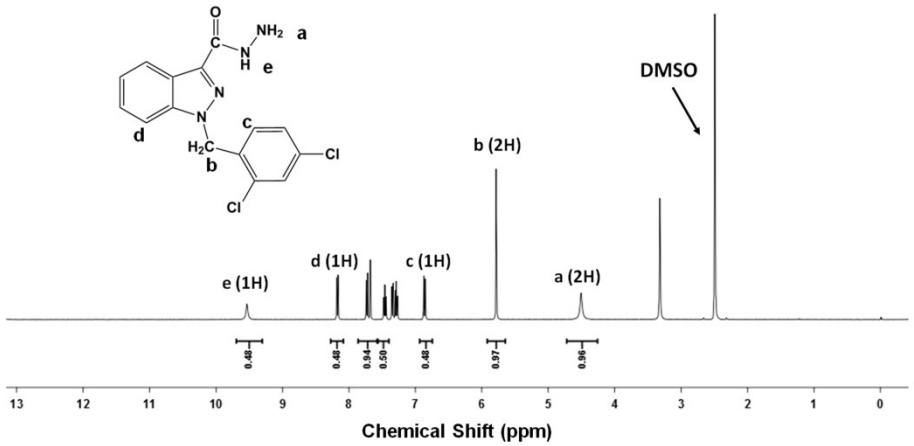

Fig. S2. ^{1}H-NMR spectrum of ADD in DMSO-d6, showing the chemical shifts of characteristic protons.

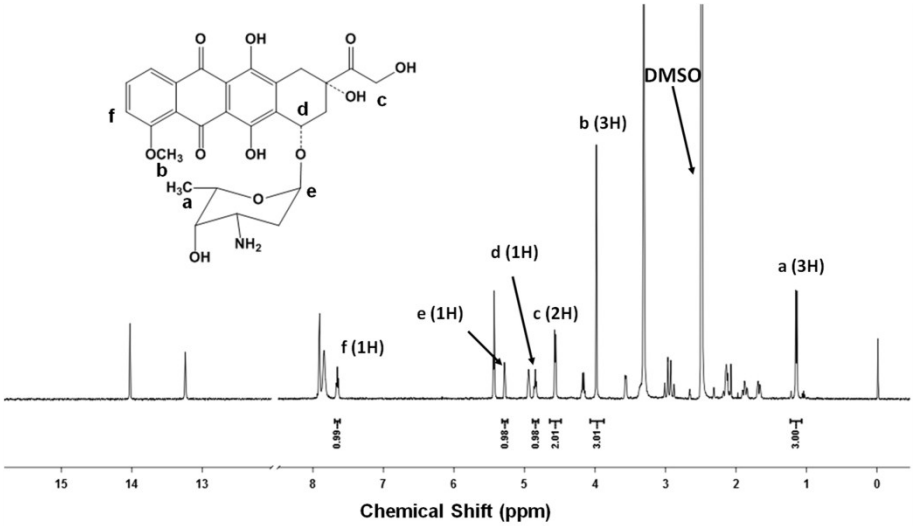

Fig. S3. ^{1}H-NMR spectrum of DOX in DMSO-d_6, showing the chemical shifts of characteristic protons.

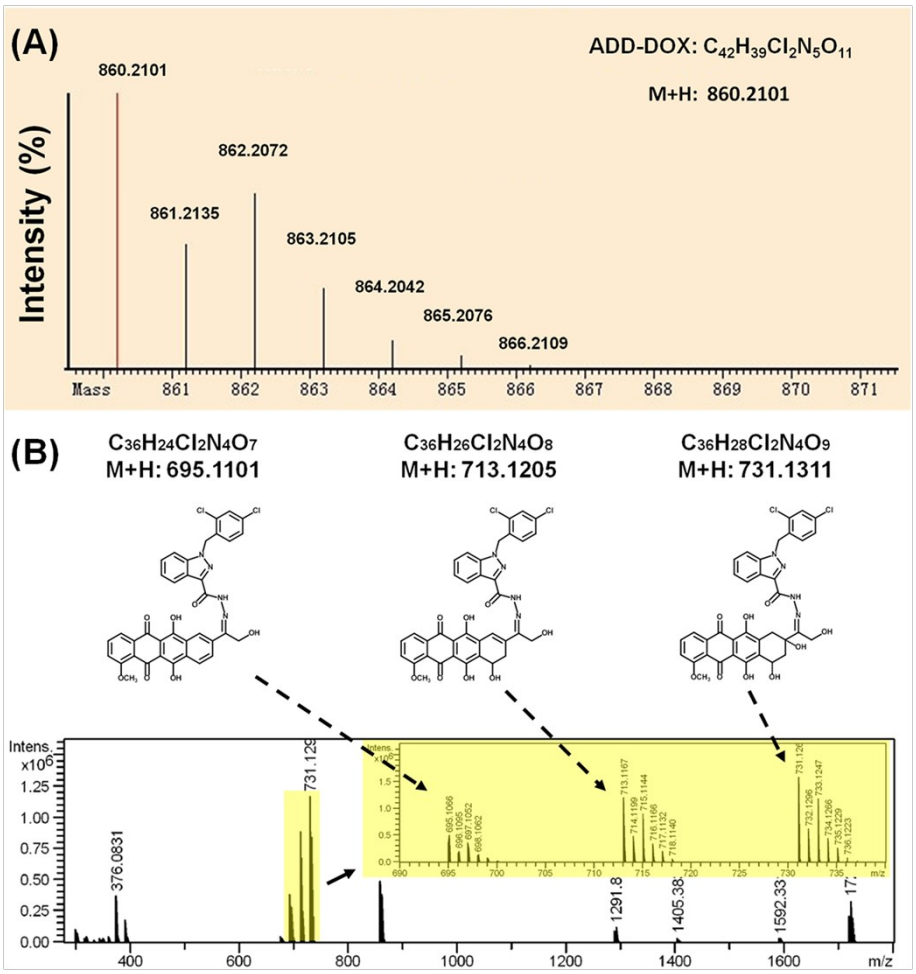

Fig. S4. (A) Theoretical isotope pattern of ADD-DOX. **(B)** HR-ESI-MS spectrum of ADD-DOX, insert (yellow) showing the expand view from 690 to 740 (m/z) and the possible corresponding molecular fragments of ADD-DOX.

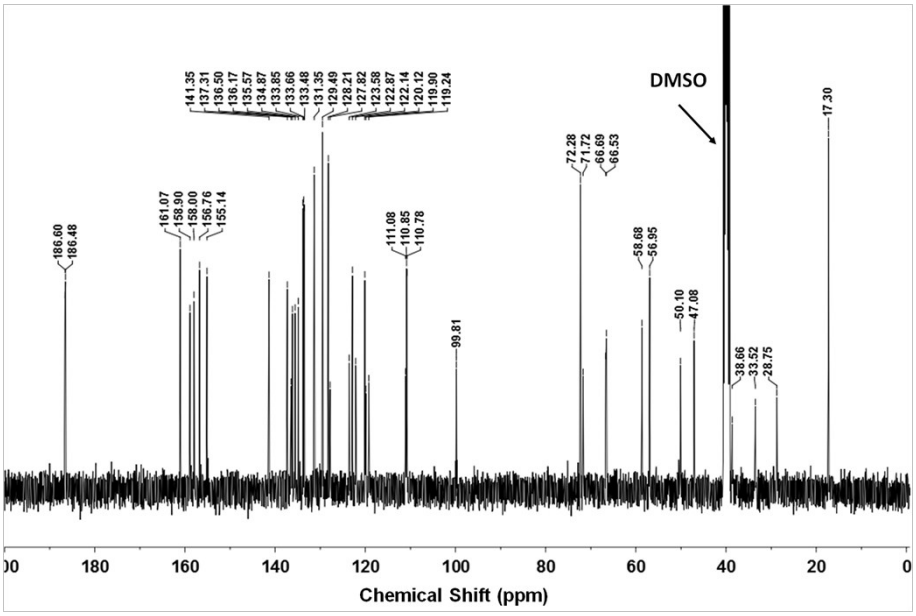

Fig. S5. ^{13}C-NMR spectrum of ADD-DOX, in which there are 42 C-related peak signals.

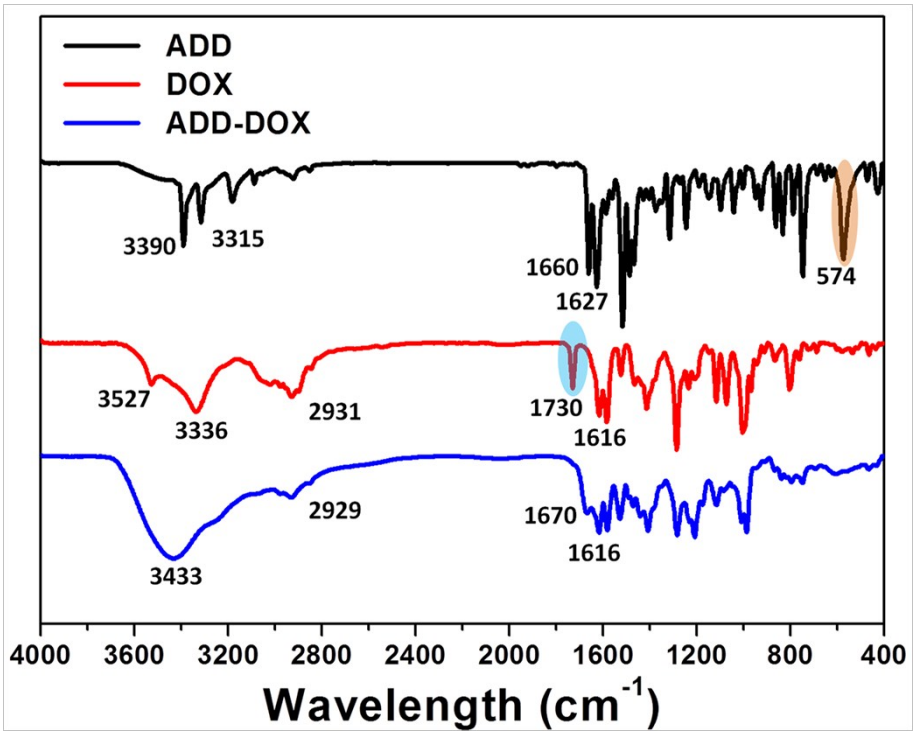

Fig. S6. Comparison the FTIR spectra of ADD, DOX and ADD-DOX.

Absorption at 574 cm^{-1} in the spectrum of ADD should be attributed to the wagging vibration of 'N-H_2' in hydrazide group (golden part). Absorption at 1730 cm^{-1} in spectra of DOX should be attributed to the stretch of carboxyl group (blue part). After the reaction of hydrazide group and carbonyl group, relative characteristic absorptions disappeared in the spectrum of ADD-DOX.

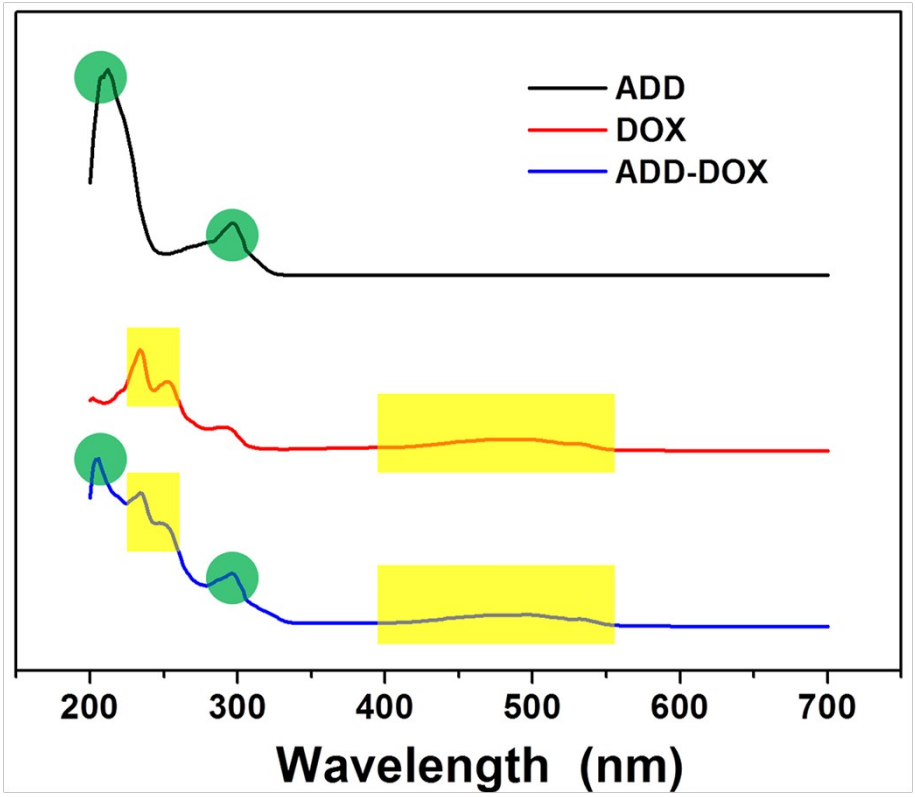

Fig. S7. Comparison of the UV spectra of ADD, DOX and ADD-DOX. Green parts indicate the corresponding characteristic absorptions for ADD and ADD-DOX (210 and 290 nm); yellow parts indicate the corresponding characteristic absorptions for DOX and ADD-DOX (230, 260 and 480 nm).

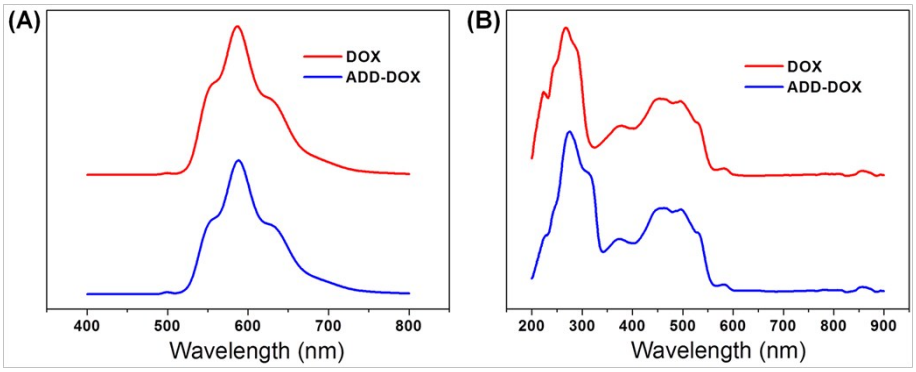

Fig. S8. Comparison of **(A)** the emission spectra with excitation wavelength of 498 nm and **(B)** the excitation spectra with emission wavelength of 588 nm of DOX and ADD-DOX in methanol, respectively (at concentration of 20 μM).

Because ADD possesses no fluorescence, we only compared the emission and excitation spectra of DOX and ADD-DOX at the same concentration of 20 μM. When fixing excitation at 498nm, the emission spectra of DOX and ADD-DOX are very similar, thus verifying that the fluorescence of ADD-DOX only attributes to the DOX moiety. When fixing emission at 588nm, the excitation spectra of DOX and ADD-DOX exhibit difference from 200-350 nm, which should be attributed to the absorption of ADD moiety in ADD-DOX.

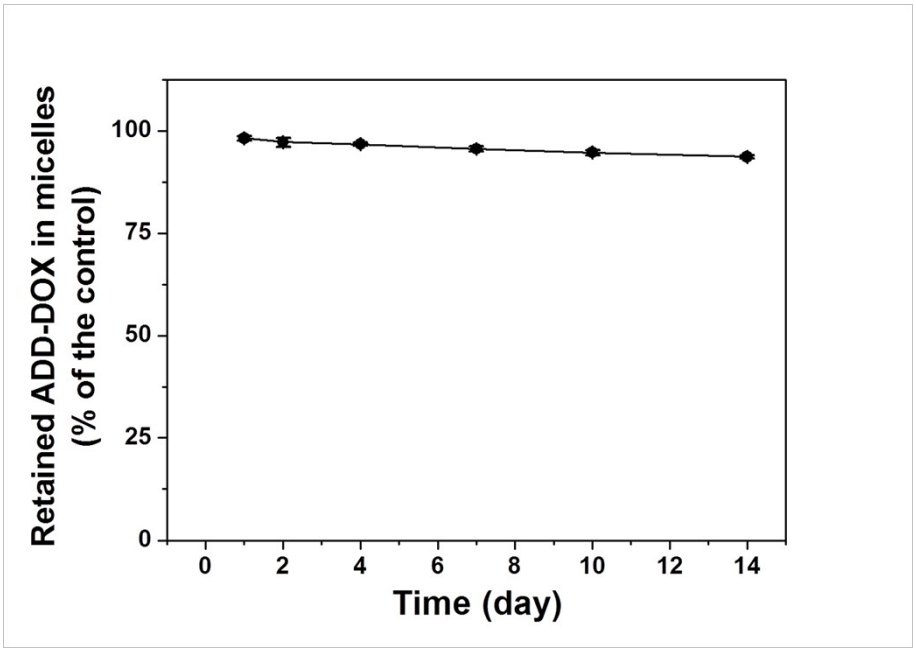

Fig. S9. Retained ADD-DOX ratio in ADD-DOX (M) storing in PBS at 4 ºC for different time periods.

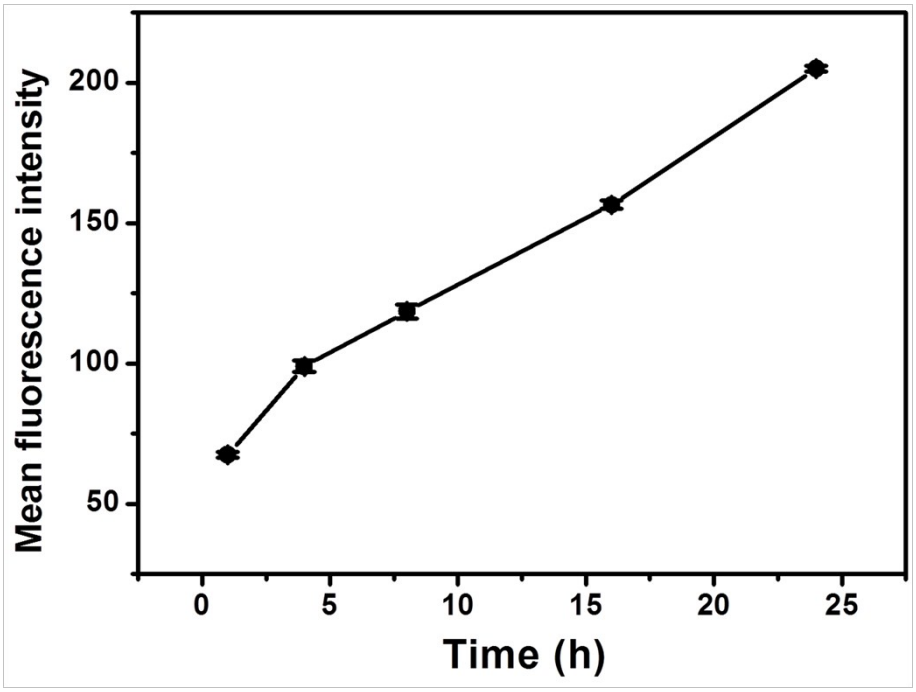

Fig. 10. Flow cytometry analysis to determine the mean fluorescence intensity (MFI) of cells incubated in medium containing ADD-DOX (M) (equivalent with ADD-DOX concentration of 5 μM) for different time periods.

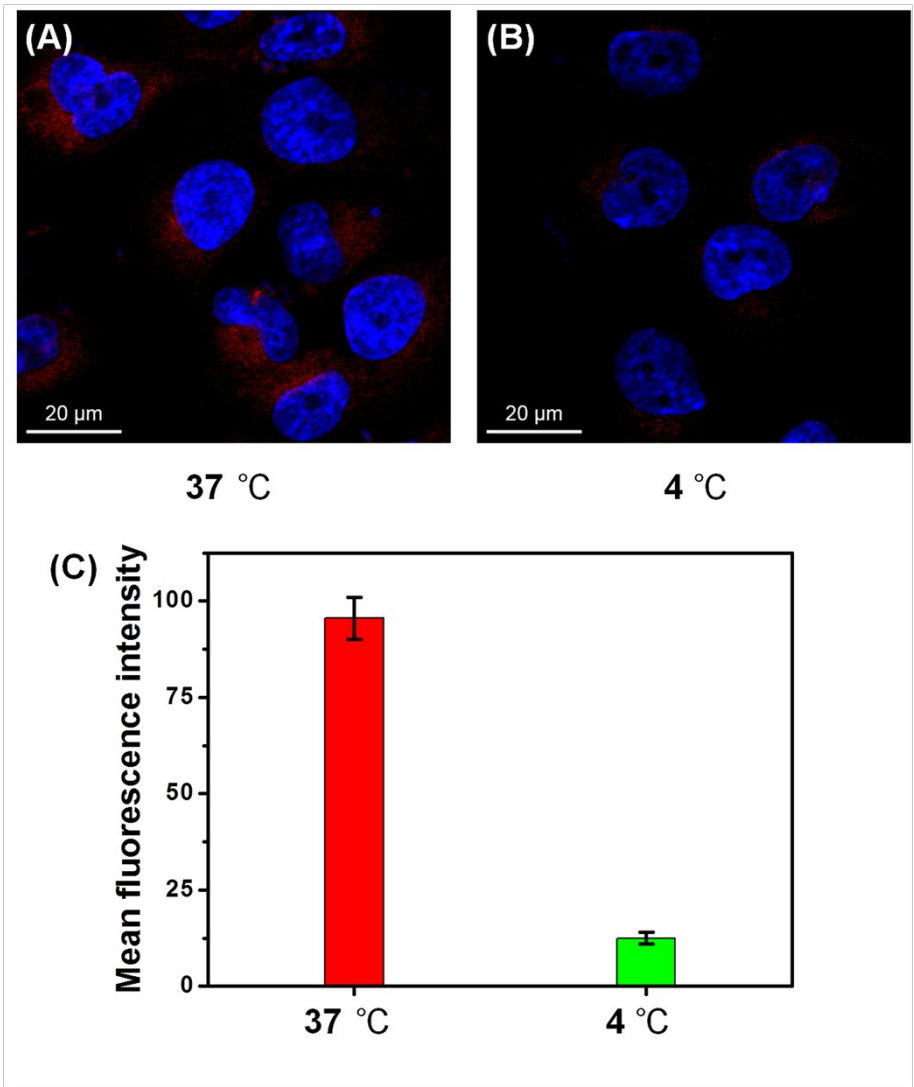

Fig. S11. CLSM images of MCF-7/ADR cells for 1h incubation with ADD-DOX (M) (equivalent with ADD-DOX concentration of 40 μM) at **(A)** 37 ºC and **(B)** 4 ºC, respectively. **(C)** Corresponding MFI determined by FCM for (A) and (B).

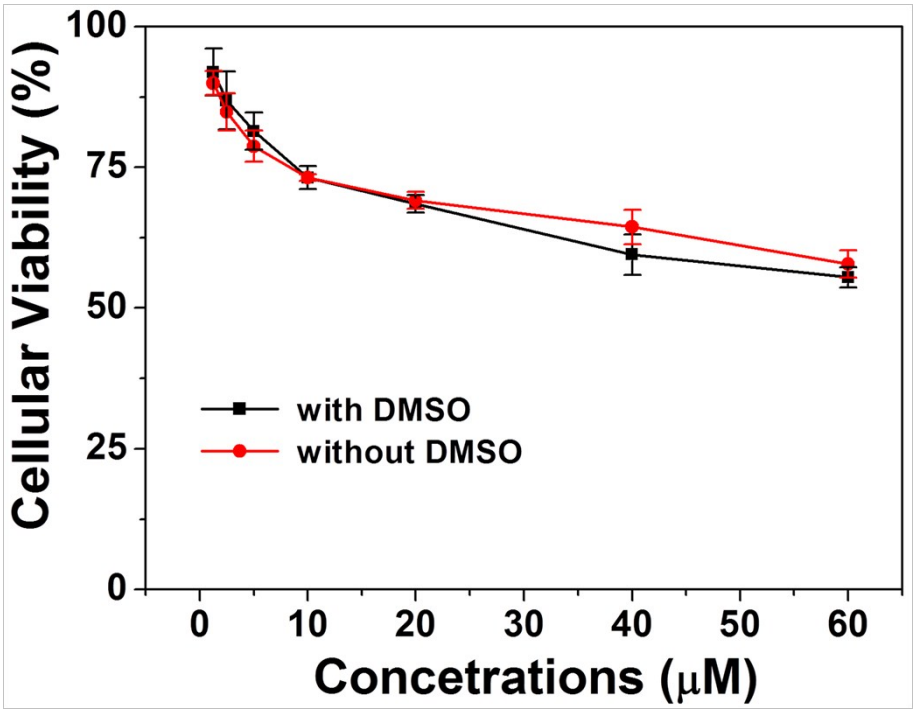

Fig. S12. Comparison of the cytotoxicity of DOX to MCF-7/ADR cells that cultured in medium with or without 0.1% (v/v) DMSO.

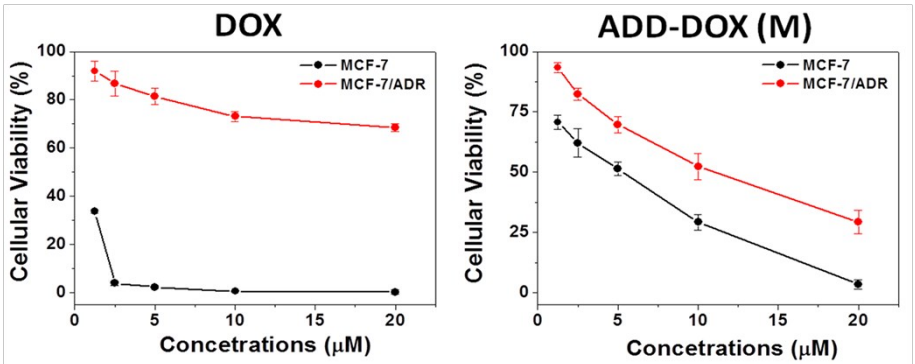

IC_{50} (μM)			
DOX		ADD-DOX (M)	
MCF-7	MCF-7/ADR	MCF-7	MCF-7/ADR
0.9	73.7	3.7	10.1

Fig. S13. Cellular viabilities of MCF-7/ADR cells or MCF-7 cells incubated with different doses of free DOX or ADD-DOX (M) for 72h.

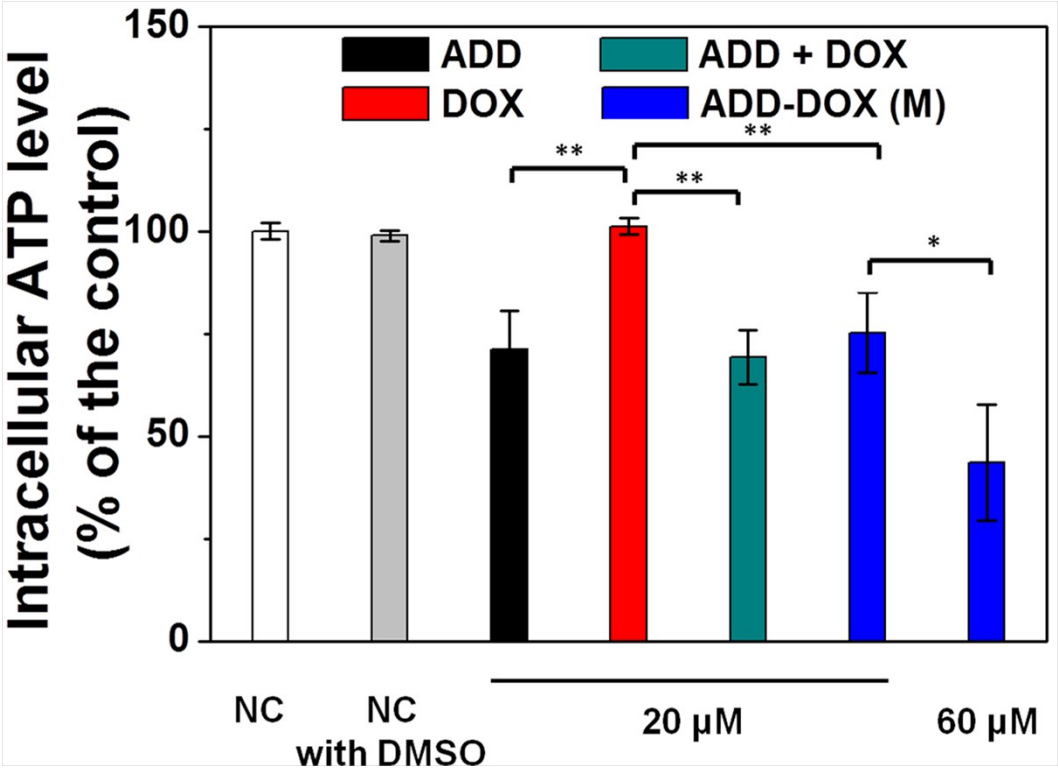

Fig. S14. Comparison of the intracellular ATP level in MCF-7/ADR cells treated by of ADD, DOX, the mixture of ADD and DOX (molar ratio of 1:1) and ADD-DOX. For the groups of applying free drugs, the cultured medium contained 0.2% (v/v) DMSO. **p<0.01, *p<0.05, n=3.

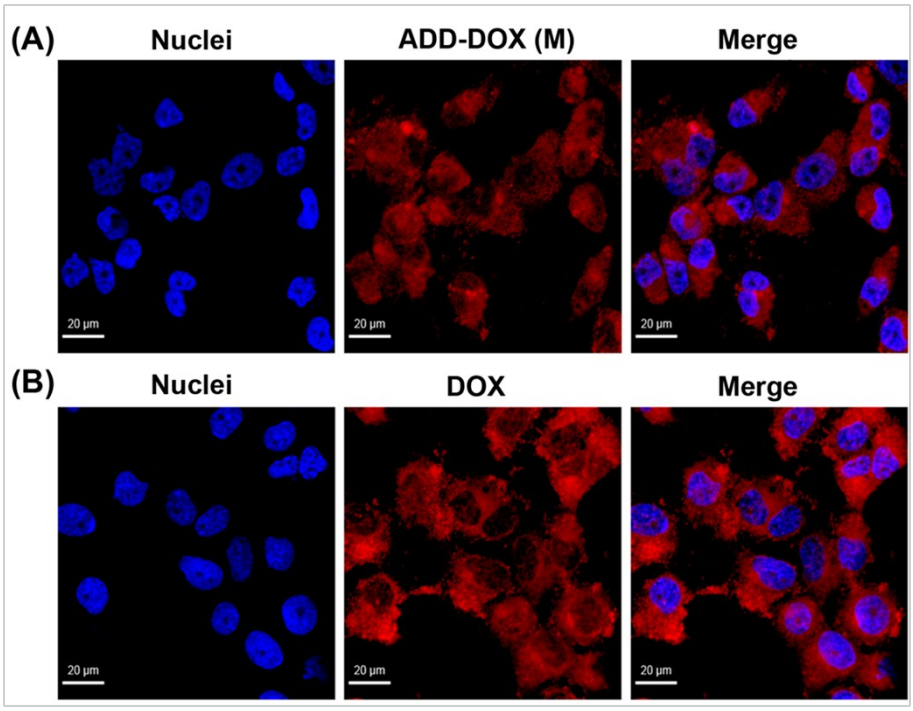

Fig. 15. Comparison of the fluorescent distribution in MCF-7/ADR cells that incubated with **(A)** ADD-DOX (M) or **(B)** DOX for 48h.